HEFAT2012
9th International Conference on Heat Transfer, Fluid Mechanics and Thermodynamics
16 - 18 July 2012
Malta

THE FEATURES OF THE LATERAL FLOW IN THE CROSS-SECTION SLICE OF AN ELONGATED BODY: EXPERIMENTAL APPROACH

Matar Y.*, Candelier F. and Solliec C.
*Author for correspondence
Department of Energetic and Environment,
GEPEA (UMR CNRS 6144)
Ecole des Mines de Nantes,
Nantes, 44300,
France,
E-mail: younes.matar@mines-nantes.fr

ABSTRACT

The aim of this work is to identify experimentally the features of the lateral flow in a cross-section slice of an elongated body during locomotion. We use an experimental approach in the context of the undulatory swimming of an elongated body. For that, two kinematic parameters of the fish's body are taking into account, the body's curvature and the cross-section diameter. We examine the lateral flow field for different elliptical cylinder-shape, and we perform the experiments using particle image velocimetry (PIV) technique.

INTRODUCTION

The Lighthill large amplitude elongated body theory (LAEBT) [1], has become one of the most fundamental theories used by the scientific communities such as biologists or bio-inspired roboticiens. In the LAEBT, it is considered that the flow in each lateral slice of the fish's body corresponds to the potential flow produced by the movement of an infinite cylinder with the same cross-section diameter. The Lighthill's 3-D model (LAEBT) referred the flow patterns in the cross-section slice of an elongated body to as "transverse" (see figure 1(b)). In contrast, in the 2-D model proposed by Wu [3], the fluid near the fish's body moves longitudinally (parallel to the direction of the swimming), it's referred to as "longitudinal" (see figure 1(a)).

Recently, the LAEBT theory has become a topic for discussion among fluid mechanicians. In particular, numerical and theoretical studies [4] - [7] have shown that the 3-D flow near the fish's body differs from that described by [1]. Reference [4] shows, through numerical simulation, that the flow near the fish's body results from a combination of "transverse" and "longitudinal" flow features along the length of the body. Furthermore, the recent theoretical work made by [7] reveals that the cross-sectional flow underlying the LAEBT is actually more complex than the 2D potential flow produced by the movement of an infinite cylinder of the same cross-section. In fact, the flow can be affected by different parameters, such as the variation of the body curvature during the lateral body's movement and the variation of the cross-section diameter along the body of the fish.

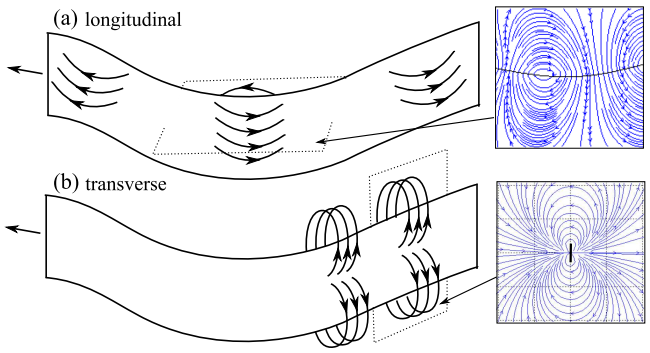

Figure 1: Flow along a straight swimming fish as modeled by: (a) 2-D swimming plate theory [3], (b) 3-D elongated slender-body theory [1]. (Figure modified from [2] and the numerical flow fields are chosen from [8])

In this study, our goal is not to dispel traditional swimming theories, but rather, to show the features of the flow around an elongated body by taking into account the

body's curvature and the cross-section area of the body. Therefore, we propose to break down the fish's swimming patterns into two distinguished movements; the forward movement of variable cross section body (see figure 2(a)), and, the lateral movement of a constant cross section area along the body's curvature (see figure 2(b)). As a result, we performed experiments on five models of elliptical cylinder-shape. Experiments are carried out in a hydrodynamic re-circulating test bench. Velocity flow fields are examined in the midplane of the lateral slice of each model by performing particle image velocimetry (PIV) technique.

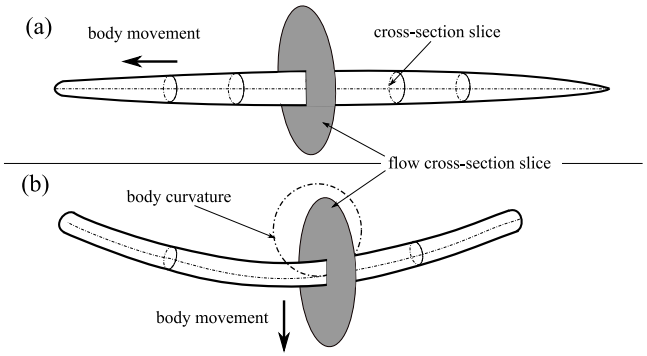

Figure 2: Sketch of two distinguished deformation of an elongated body during swimming.

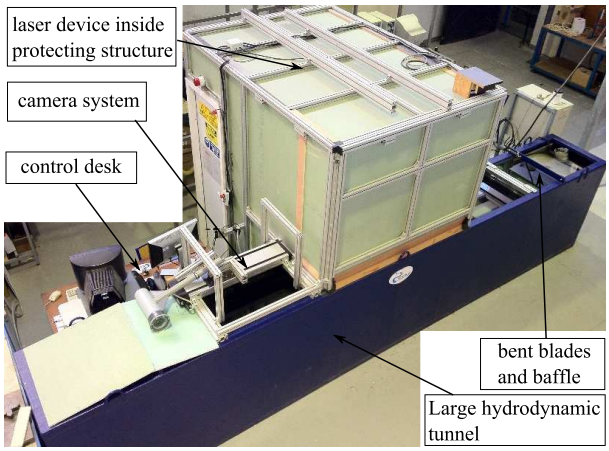

Figure 3: Photography of the hydrodynamic test bench with different components.

Table 1: Characteristics of the elliptical cylinders-shape

Model	β	α	R	K	γ
C_1	1	0.67	∞	0	0.1
C_2	1	0.67	∞	0	0
C_3	1	0.67	3.33	0.3	0
C_4	1	0.67	2.67	0.375	0
C_5	1	0.67	2	0.5	0

Non-dimension parameters

MATERIALS AND METHODS

Hydrodynamic Test Bench

Experiments were performed in a re-circulating hydrodynamic test bench. This bench is composed of a large tank (6 m × 0.8 m × 1.2 m) separated in two parts by two large parallel plates. A variable-speed axial turbine was used to set the flow velocity in the channel; it can be set up from 0 to 0.5 m/s. In order to reduce the turbulence of the incoming flow, two bent blades and baffle of flow straighteners were placed at the end of the tank, downstream the turbine. Figure 3 shows the photograph of the hydrodynamic test bench.

Elliptical Cylinder Models

The elliptical cylinder models were designed using the CATIA CAD software. They were manufactured from transparent plastic material using prototype Injection Molding Process.

Experiments were carried out on five elliptical cylinder-shaped. The first one (C_1 cylinder) has a variable elliptical cross-section with infinite radius of the curvature. The four other models (C_2 up to C_5) have the same cross-section diameter with variable curvature's radius from one to another. A summary of the characteristics of each model is provided in the Table 1, and all dimensions are normalised with respect to the major axis (45 mm). In addition, in the figure 4, we see a 2-D dimensional sketch (top and back view, dimension in mm) of the two elliptical cylinders C_1 and C_3, and in the figure 5, the photography of the actual models. We define β as the major axis, α as minor axis, R as the radius of the curvature, K is equal to $1/R$ the inverse of the radius of curvature and γ is equal to $\partial\beta/\partial x = \partial\alpha/\partial x$ (x represent the coordinate along the axis of the cylinder).

Experimental Apparatus and PIV Setup

An overview of the experimental apparatus is presented in the figure 6. The experiment was performed in a 3 m x 0.5 m x 0.7 m working section using PIV.

The pulse laser device (newWave Solo Nd:Yag 120 mJ pulses @ 15 Hz, Wavelength 532 nm) is mounted on two perpendicular traverse in a way that the laser sheet is perpendicular to the direction of the flow (perpendicular to the elliptical cylinder). The laser device can move in two perpendicular directions. In order to insure that the laser sheet is perpendicular to the cylinder, the laser sheet must be perpendicular to the light sheet reflected from the tank wall.

The Dantec HiSense camera with 1600 x 1200 pixels is equipped with a 50 mm focal length lenses and green light filters. It is immerged in water using a waterproof camera box made with a transparent plastic material based on the front side of the camera. The camera is mounted on

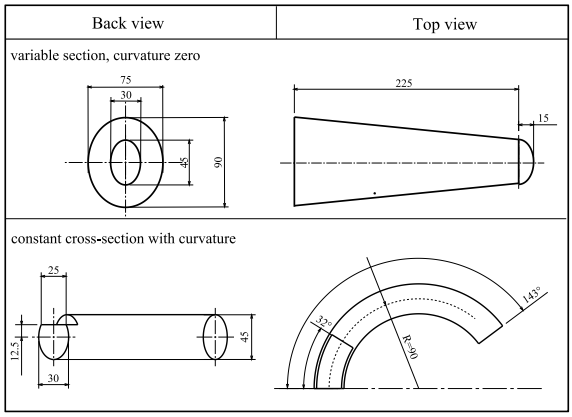

Figure 4: 2-D dimentional sketch from CAD drawing C_1 is the first model and C_2 is the next one.

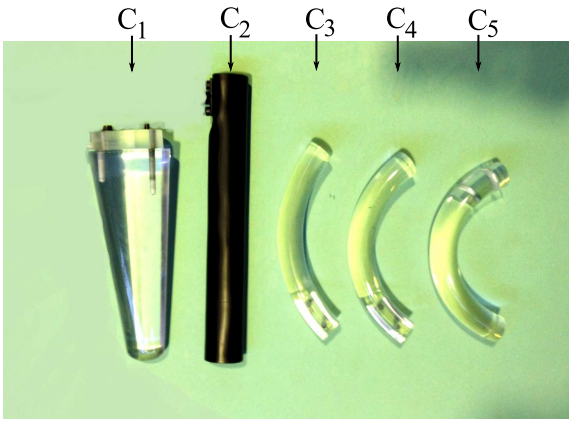

Figure 5: Photography of the actual models.

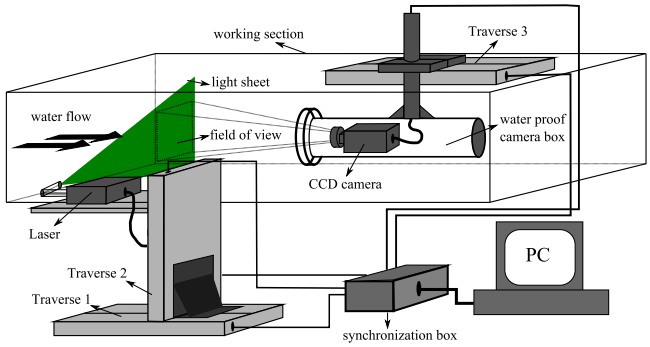

Figure 6: Schematic view of the experimental apparatus.

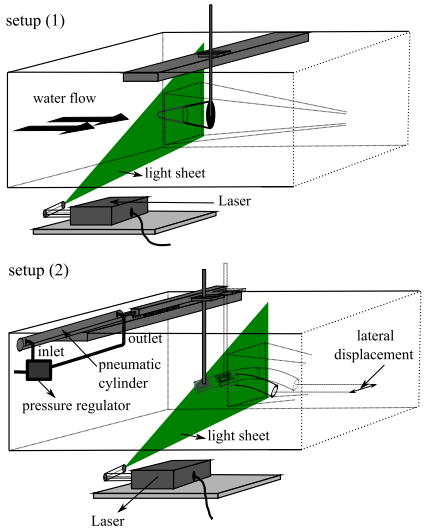

Figure 7: Schematic view of the two experimental setups

the traverse and moves in a parallel direction to the laser device's movement in order to have a fixed position relative to one another. Water flow was seeded using 25μm polyamide particles. Dantec DynamicStudio software is used for PIV measurements and data processing.

Experimental Procedure

PIV measurements were performed using two experimental setups. They are referred in figure 7 as setup (1) and (2).

In the first one, the elliptical cylinder C_1 was fixed to a vertical metal rod, in a manner that the symmetric horizontal axis of the cylinder is set parallel to the direction of the flow, and that the circular side is placed against the flow's direction. Measurements were carried out in the vertical midplane of the cylinder.

In the second one, the measurements were performed in the hydrodynamic tunnel without velocity flow. To insure the lateral movement of the elliptical cylinders (C_2 - C_5), a pneumatic cylinder system was used. Each cylinder was fixed to a metal rod, which was in turn fixed to the extremity of the piston road. The movement is assumed to be linear with 250 mm stroke range at constant speed.

As a result, velocity vectors grids and streamlines are obtained in the midplane cross-section of each model by performing cross-correlation analysis and data processing on the recorded images from PIV measurements.

RESULTS AND DISCUSSIONS

During the swimming of an elongated body, the propulsion is insured by the travelling of a deformation wave along the body, and whose amplitude increases gradually from head to tail. Near the head, the lateral flow velocities of an elongated body with variable cross-sections are generally small compared to the axial velocity, and the local curvature of the body is often negligible [7]. In contrast, near the tail, the local curvature may become significant, and the body cross-section area can be considered as constant. So the lateral flow features differ in the cross-section slice along the body from the head to the tail. Therefore, in order to understand the surrounding flow features of the swimming of an elongated body, streamlines and velocity vectors grids which were obtained experimentally

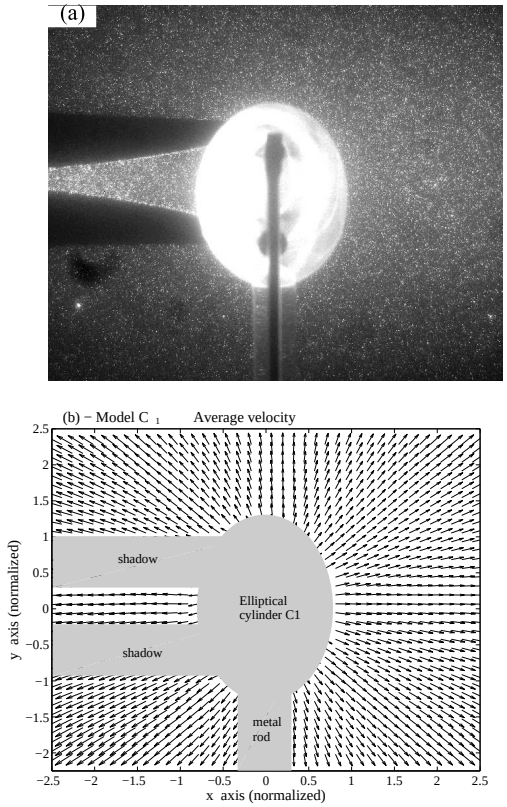

Figure 8: Experimental velocity field captured using particle image velocimetry PIV in the midplane cross-section of the cylinder C_1: image signal provided by the CCD camera (a), and, normalized average velocity vector from 1500 double-frame samples (b).

are presented in the following section.

Variable Section

In this section, the lateral flow pattern of the variable cross-section cylinder is provided. The cylinder C_1 was fixed in the opposite direction of the velocity flow. The velocity of the incoming flow defined by U is equal to 0.285 m/s. In the figure 8 we show, an arbitrary image signal provided by the CCD camera (figure 8(a)) and the average velocity vector field from 1500 double-frame samples (figure 8(b)).

When the fluid goes through the cylinder C_1, the cylinder pushes surrounding fluid laterally, as illustrated by the direction of the black arrow in the figure 8 (b). The mean of the lateral velocity represents 0.2 % from the axial velocity U and it is shown to be normalised with respect to U.

Variable Curvature

Now, the lateral flow in the midplane cross-section slice of the cylinders C_2, C_3, C_4 and C_5 are studied. The speed of the lateral displacement of the elliptical cylinders defined by V is approximately equal to 0.48 m/s. Figure

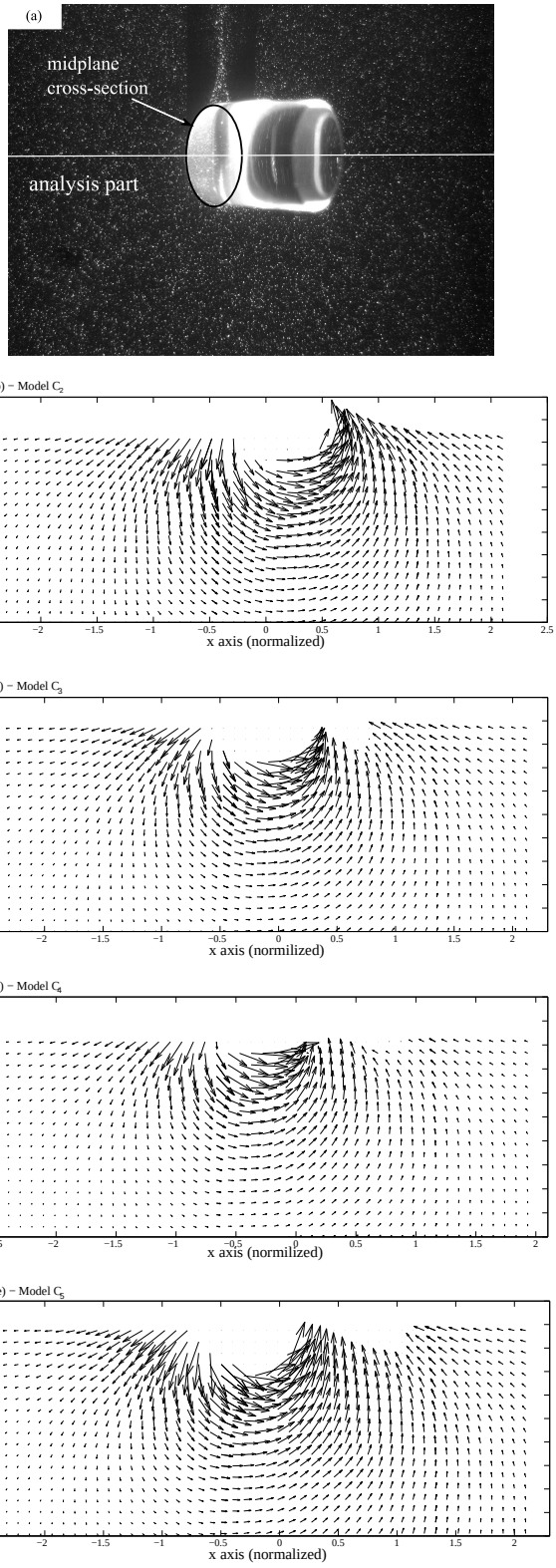

Figure 9: Experimental velocity field captured using particle image velocimetry PIV in the midplane cross-section of the cylinders $C_2 - C_5$: sample of image signal provided by the CCD camera (a), and, the normalized instantaneous velocity vector of the lateral flow of the cylinders C_2 - C_5 (b)-(e).

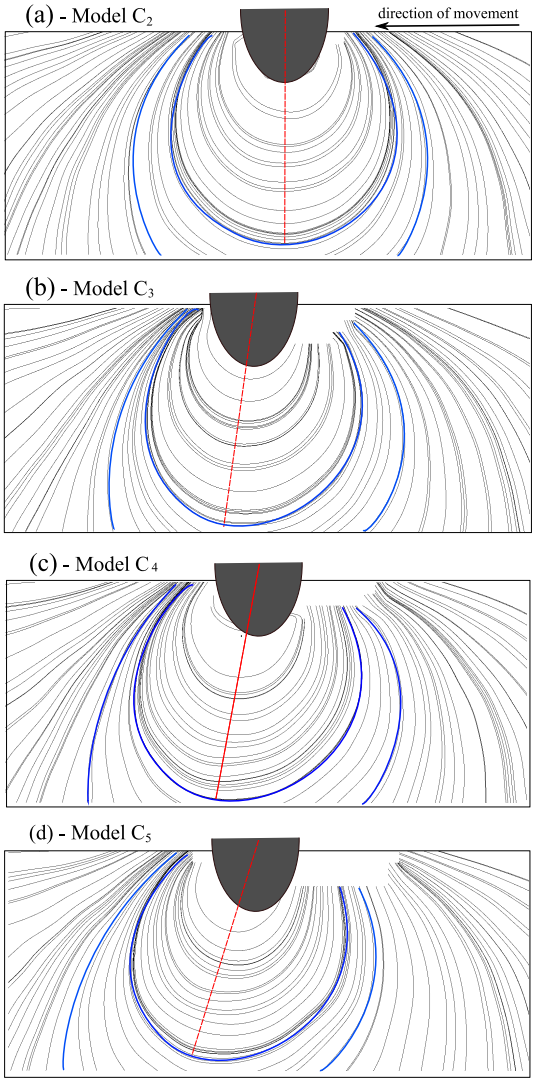

Figure 10: Streamlines representation of the same informations presented in the figure 9.

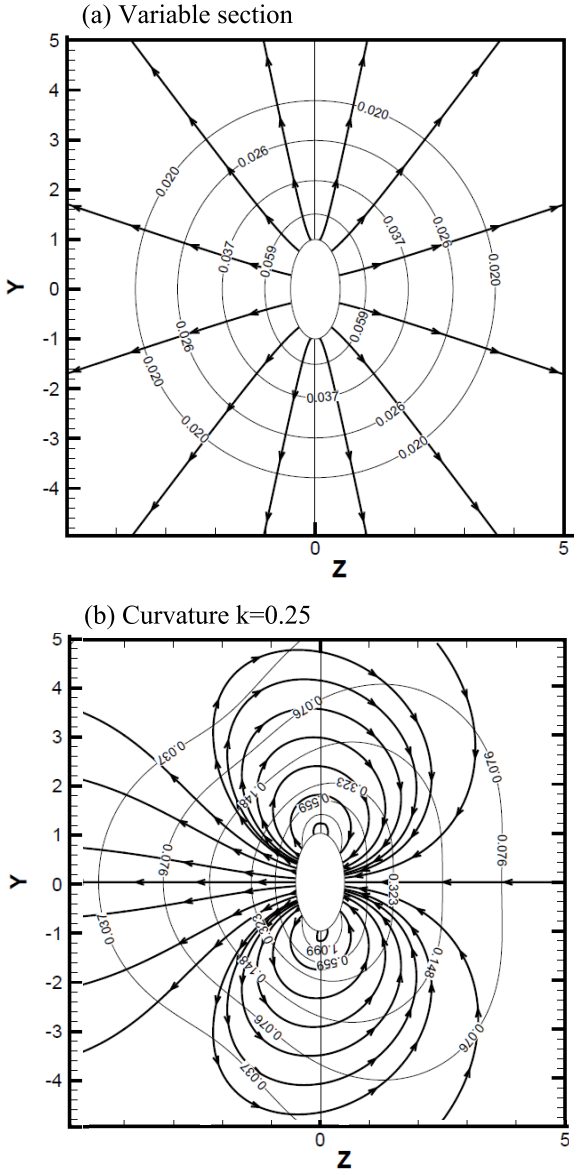

Figure 11: Streamlines of the lateral flow presented by [7]: the radial flow during the axial movement of an elliptical cylinder with variable cross-section (a), and the transverse flow during the lateral movement of an elliptical cylinder with normalized curvature equal to 0.25 (b).

9(b), (c), (d) and (e) shows the normalised (with respect to V) instantaneous velocity flow fields that correspond respectively to the lateral flow of the cylinders C_2, C_3, C_4 and C_5. The direction of the cylinder motion is from the right to the left. Only the lower part of the PIV image signal is analysed (see figure 9(a)). In order to show clearly the lateral flow patterns, the same informations of the figure 9 are presented as streamlines in the figure 10.

We can see from the first observation of these results, a significant difference between the flow pattern of the cylinder C_2 and the others. In the potential flow around the cylinder C_2, the streamlines have a symmetrical shape with respect to the red line (see figure10 (a)). In contrast, in the lateral flow of the cylinders with curvature different to zero, the streamlines patterns are not symmetric anymore, and the deviation of the red line increases when body curvature increases (see figure 10(b), (c) and (d)).

Note that the pattern of the streamlines and the velocity vector field can be qualitatively compared with good agreement with the numerical and theoretical studies presented respectively by [4] and [7]. Figure 11 shows the streamlines of the lateral flow presented by [7]; (a) the axial movement of an elliptical cylinder with variable cross-section and (b) the lateral mouvement of an elliptical cylinder with curvature (normalized with respect to the half of the major axis β) equal to 0.25.

We can deduce that the feature of the lateral flow in a cross-section slice of an elongated body is more complex than the 2-D potential flow of an infinite cylinder proposed

by [1]. Indeed, the body curvature and the cross-section area have a significant influence on the pattern of the flow surrounding the body of the fish while it's swimming.

CONCLUSION

This paper provides experimental results of the features of the lateral flow in the cross-section slice of an elongated body. We propose an experimental approach in order to understand the nature of the fluid around the body of the fish, by taking into account the variation of the cross-section area and the curvature of the body. We performed experiments on five elliptical cylinder shapes. We observed that when the fish moves its body axially, it pushes the surrounding fluid laterally. In addition, when the body moves in a lateral direction with constant cross-section area, the body curvature changes and the flow patterns, in the cross-section slice, differ from the 2-D potential flow proposed in the LAEBT Lighthill theory. We have deduced that the body curvature and the cross-section body area have a significant influence on the features of the flow surrounding the body of the fish.

ACKNOWLEDGMENT

This study was supported by the European Commission, Information Society and Media, Future and Emerging Technologies (FET) contract 231845.

References

[1] Lighthill J., Large-amplitude elongated body theory of fish locomotion, *Journal of Fluid Mechanic*, 1971, pp. 125-138.

[2] Anderson J. M., Vorticity Control for Efficient Propulsion, PhD thesis, *Massachsetts Institute of technology*,1996.

[3] Wu T. Y-T., Swimming of a waving plate, *Journal of Fluid Mechanic*, Sept 1961, pp. 321-355.

[4] Wolfgang M. J., Anderson J. M., Grosenbaugh M. A., Yue D. K. P., Triantafyllou M.S., Near-Body flow dynamics in swimming fish, *Journal of Experimental Biology*, May 1999, pp. 2303-2327.

[5] Wolfgang, M. J., Hydrodynamics of flexible-body swimming motions, PhD thesis, *Massachsetts Institute of technology*,1999.

[6] Zhu Q., Wolfgang, M. J., and Triantafyllou, M. S., Three-dimensional flow structures and vorticity control in fish-like swimming, *Journal of Fluid Mechanic*, Marsh 2002, pp. 1-28.

[7] Candelier F., Boyer F., and Leroyer A., Three-dimensional extension of the Lighthill's large-amplitude elongated-body theory of fish locomotion, *Journal of Fluid Mechanic*, Marsh 2011, pp. 196-226.

[8] Porez M., Modèle dynamique analytique de la nage tridimensionnelle anguilliforme pour la robotique., PhD thesis, *Ecole des Mines de Nantes*,1996.